Available online at www.sciencedirect.com
SCIENCE DIRECT®
Electrochimica Acta 49 (2004) 745–752
ELECTROCHIMICA Acta
www.elsevier.com/locate/electacta

Dynamic behaviour of viologen-activated nanostructured TiO_2: correlation between kinetics of charging and coloration

Jorge Garcia-Cañadas [a], Francisco Fabregat-Santiago [a,*], Jon Kapla [b], Juan Bisquert [a], Germà Garcia-Belmonte [a], Ivan Mora-Seró [a], Marten O.M. Edwards [b]

[a] *Departament de Ciències Experimentals, Universitat Jaume I, 12080 Castelló, Spain*
[b] *Department of Physical Chemistry, Uppsala University, Box 579, 75123 Uppsala, Sweden*

Received 29 May 2003; received in revised form 19 September 2003; accepted 28 September 2003

Abstract

The dynamic response of viologen-activated nanostructured titanium dioxide has been studied by means of electrical and electro-optical measurements. We show that the state of charge of the semiconductor network is the key factor mediating between the electrode potential and colouration of viologen. Theoretically, we relate the electrode potential to the statistics of occupancy of both TiO_2 nanoparticles and oxidized viologen molecules attached to the surface, on the assumption of quasi-equilibrium of Fermi levels in these contacting phases. Experimentally, we determine the statistical function from steady-state measurements (electrochemical impedance spectroscopy) of the capacitance of the semiconductor film. From this understanding we explain the main features that correlate the simultaneous voltammetry and transmittance responses. Finally, the redox process of viologen is resolved separately from the TiO_2 response by means of transmittance data.
© 2003 Elsevier Ltd. All rights reserved.

Keywords: Charging and coloration; Viologen; Nanostructured TiO_2; Electrochromism

1. Introduction

Viologen-modified nanostructured TiO_2 films have recently attracted attention as suitable electrodes for electrochromic applications. Such devices present rapid switching between the bleached and coloured states, high contrast ratios and good cycling stability [1]. Viologens (1,1′-disubstituited 4,4′-bipyridinium) work as electrochrome. The first reduction of the viologen molecules is highly reversible and leads to the formation of the intensely deep blue coloured radical cation [2]. The devices rely on the fast interfacial electron transfer between the nanocrystalline oxide and the adsorbed modifier as well as on the high surface area of the nanocrystalline support, which amplifies optical phenomena by two or three orders of magnitude [3]. Electrical and optical studies on the dynamics of viologen-modified nanostructured TiO_2 electrode have been reported recently [4,5].

Besides stability, major issues in the electrochemical characterization of viologen modified mesoporous electrodes are the relation of colouring with the applied potential and the kinetics of the colouring process. Provided that high speeds of electron transfer both to the TiO_2 nanostructure, and between the oxide surface and attached molecules, are obtained, the crucial factor controlling the colouration is the charge density in the nanoporous network at each potential. Recent insights related to dye-sensitized solar cells studies provide a quantitative control of the relationship of electron accumulation in TiO_2 nanoparticles to the electrode potential. For instance it was shown that the electron conductivity of the semiconductor, when separated from electrolyte components, correlates exponentially with the electrode potential [6]. Similar concepts enable a qualitative understanding and a quantitative description of capacitance and interfacial charge transfer of nanostructured TiO_2 electrodes using steady-state electrochemical impedance spectroscopy (EIS) [7] and transient electrical currents in response to a large amplitude voltage scan at a constant rate (voltammetry) [8].

It is natural to apply these developments to the kinetics of viologen modified mesoporous electrodes, and that is the aim of this paper. We start from the idea that the opacity

* Corresponding author. Tel.: +34-964-728024; fax: +34-964-728066.
E-mail address: fabresan@exp.uji.es (F. Fabregat-Santiago).
URL: http://www.elp.uji.es.

0013-4686/$ – see front matter © 2003 Elsevier Ltd. All rights reserved.
doi:10.1016/j.electacta.2003.09.028

of the film will be determined by electron density in the semiconductor nanoparticles. Some insights in this direction were obtained in [4], where the response of different electrical and electro-optical small perturbation frequency techniques enabled to follow the dynamic relation of the electron concentration at the same time as the electrochromic effect. Here, the charging of the nanoparticles with respect to stationary or time-varying voltage will be determined with the new tools developed previously for the unmodified nanostructured electrode [7,8]. On the basis of nearly reversible interfacial charge transfer, and with suitable assumptions on the redox process occurring at the molecules attached at the particles surface, transients of transmittance and the kinetics of colouration in general will be described.

Our strategy is to use the steady-state frequency technique information (EIS) as an input for describing the correlation of the response of large amplitude electrical and electro-optical time transient techniques (i.e. voltammetries and simultaneous transmittance). We first characterize the capacitance of the device as function of potential by means of EIS, identifying the contribution of the different elements in the film that dominate at each voltage region. These features will be subsequently used to interpret the voltammogrames and transmittance transients that are obtained when the adsorbed viologen is reduced and oxidized during a potential scan. The quantitative contribution of the viologen molecules to electrical transients is estimated and finally, the redox process of viologen is decoupled completely from the TiO_2 response and depicted separately by means of transmittance data.

2. Experimental

The viologen bis(2-phosphonoethyl)-4,4′-bipyridinium dichloride was synthesised as described by Cummins et al. [1]. Conductive glass substrates (Hartford glass, TEC8, fluorine-doped SnO_2, from now FTO) were cleaned by rinsing with 99% EtOH and dried in air. Colloidal solution of nanocrystalline TiO_2 (particle size of 10–14 nm), was spread over the cleaned conductive glass surface with a glass rod, using single layers of Scotch tape as spacers and fired at 450 °C for 30 min in air. Immediately after cooling the samples were immersed in a 0.5 mM solution of viologen in methanol. Chemisorption of viologen onto the TiO_2 surface was allowed to proceed overnight, and then the samples were taken out from the solution and dried in air. Two TiO_2 samples of the same batch were used in this study: the first one was derivatised with viologen while the second was kept free to be used for blank measurements. Their geometric areas were 1 and 0.68 cm^2, respectively and their average thickness 4 μm.

Electrochemical measurements were carried out in a three-electrode cell under nitrogen. A Ag/AgCl/KCl (3 M) reference electrode was connected to the cell by means of a salt bridge containing the electrolyte solution and a Pt wire was used as counter electrode. The electrolyte solution was 0.2 M lithium triflate (Aldrich) in 3-methoxypropionitrile (Aldrich). Voltammetric and EIS measurements were performed using an Autolab PGSTAT 20. For the impedance measurements, the potential modulation was 10 mV and the frequency ranged from 1 kHz to 5 mHz. The optical transmittance was measured simultaneously to the votammetries by illuminating the cell from the substrate side with a He–Ne laser (wavelength 543.5 nm) and collecting the transmitted light with a silicon photodetector.

3. Results and discussion

A series of EIS measurements was done at different steady-state potentials (between 0 and −1 V versus Ag/AgCl) over bare and viologen modified nanoporous TiO_2 films. The impedance spectra of the samples at the lower and higher potentials had the same shape, in both cases, as that shown in Fig. 1(a). This response may be roughly modelled, as it was done previously [4,5], by the series connection of a resistance, R, and a capacitance, C, being this C the low frequency limit of the capacitance that can be extrapolated from the capacitance spectra, Fig. 1(b). In the region of intermediate potentials, between −0.2 and −0.4 V, due to the effect of the transport resistance of the

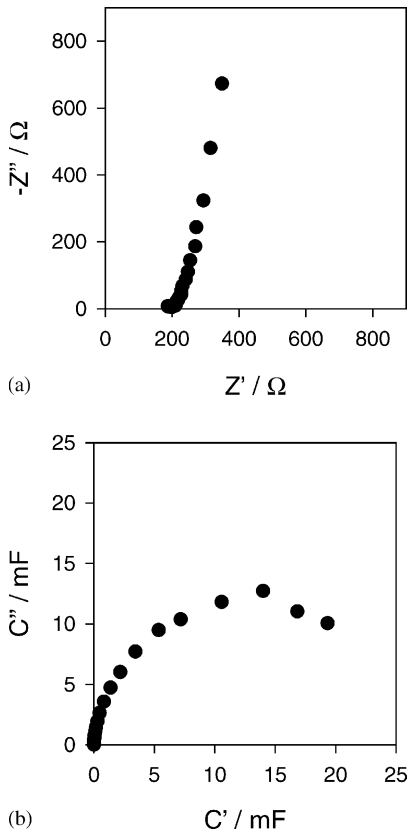

Fig. 1. (a) Impedance spectra of a viologen modified TiO_2 at −0.6 V vs. Ag/AgCl. (b) The same in the capacitive representation.

semiconductor, a more refined (and complex) model, similar to the one used on bare TiO_2 in water of [7], is needed to fit correctly the data. However, in a further work [8], it was shown that the corrections due to this transport resistance had a minor effect on the results of voltammetry, being the low frequency elements of EIS, in our case the capacitance and the series resistance, the ones that dominate the voltammetries in this region.

From the fits to this simple RC equivalent circuit of both bare and viologen-activated TiO_2, we obtained a series resistance of 200 Ω, which is the sum of the FTO (∼40 Ω) and electrolyte resistances, and the voltage dependent capacitances shown in Fig. 2(a). Note that in [5] the variations of these capacitances represented in Fig. 2(a) are approximated with a step function.

The interpretation of the different components of the capacitance is indicated in the scheme of Fig. 2(b). In the region of positive potentials, at which the TiO_2 matrix is insulating, the observed capacitance is due to the Helmholtz layer at the uncovered FTO bottom substrate [9] and it is nearly the same in both, the bare and the covered cases. At more negative potentials, when electrons are injected in TiO_2, the capacitance of the film rises exponentially with the applied voltage, void circles in Fig. 2(a), what has been previously identified for bare TiO_2 electrodes in water as a process of accumulation of charge in the semiconductor [7,8].

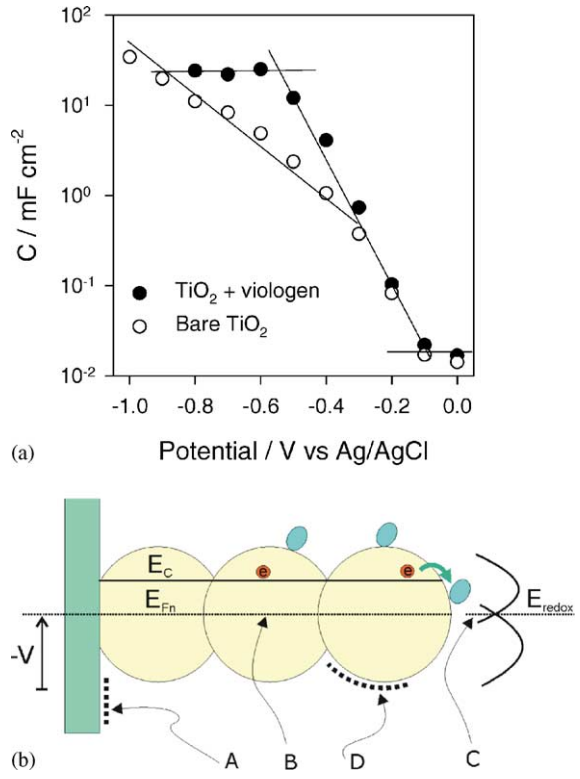

Fig. 2. (a) Capacitance of bare (○) and viologen-activated TiO_2 (●) obtained from EIS measurements. The lines are a guide to indicate different domains of behaviour. (b) Scheme of a nanoporous electrode with attached viologen molecules, showing the different capacitive processes that contribute to the experimental response. (A) Capacitance of the Helmholtz layer at the interface between the exposed surface of the conducting substrate and the electrolyte. (B) Chemical capacitance due to increasing chemical potential (concentration) of electrons in the TiO_2 phase, obtained when the electrode potential, V, displaces the electron Fermi level, E_{Fn}, with respect to the lower edge of the conduction band, E_c, in the semiconductor nanoparticles. (C) Chemical capacitance due to the redox process occurring when the semiconductor Fermi level, E_{Fn}, displaces the redox potential, E_{redox}, of the viologen molecules. (D) Constant Helmholtz capacitance at the oxide/electrolyte interface.

We summarize in the following the interpretation of this capacitance: assuming that the contact of TiO_2 nanoparticles with the substrate is ohmic, the local electrochemical potential of electrons at the conducting substrate, $-eV$ (where e is the elementary charge, and V the substrate potential measured with respect to a reference in solution), and the Fermi level in the semiconductor network, E_{Fn}, are related simply as $-e\mathrm{d}V = \mathrm{d}E_{Fn}$ [8]. The capacitance per unit volume in the semiconductor network ($C = -\mathrm{d}Q/\mathrm{d}V$), corresponding to the Fermi level displacement with respect to the conduction band, Fig. 2(b), is, therefore

$$C_{TiO_2} = -e\frac{\mathrm{d}n}{\mathrm{d}V} = e^2\frac{\mathrm{d}n}{\mathrm{d}E_{Fn}} \quad (1)$$

with n the electron density in the semiconductor. Eq. (1) corresponds to a chemical capacitance that can be defined from quite basic thermodynamic considerations [10]. In general the chemical capacitance is $C = e^2\partial N_i/\partial\mu_i$ and reflects the capability of a system to accept or release additional carriers with density N_i on a given variation of their chemical potential, μ_i. In the semiconductor network, the statistics of electrons is described by the expression

$$E_{Fn} = E_{cb} + k_B T \ln\frac{n}{N_c} \quad (2)$$

where E_{cb} is the energy of the lower edge of the conduction band, N_c the effective density of states in the conduction band, k_B Boltzmann constant and T the temperature. Using Eq. (2), the chemical capacitance of Eq. (1) takes the form

$$C_{TiO_2} = \frac{e^2}{k_B T}n \quad (3)$$

With the identity $E_{Fn} - E_{F0} = -e(V - V_0)$, that relates the Fermi level and electrode potential to equilibrium values indicated by subscript 0, the electron density can be expressed $n = n_0 e^{-\alpha e(V-V_0)/k_B T}$, where $\alpha \leq 1$ is an additional constant accounting for bandgap localized states [8]. In conclusion Eq. (3) gives an exponential dependence of the capacitance with respect to the electrode potential.

In order to interpret the capacitance it is also important to take into account that electron charge is transferred from the semiconductor to the viologen molecules adsorbed in the TiO_2 surface. Let c_{red} and c_{ox} denote the concentration (in cm^{-3}) of reduced and oxidized molecules, with $c_{tot} = c_{red} + c_{ox}$. The reduction of viologen molecules is determined by the redox level defined as

$$E_{redox} = E^{(0)}_{redox} + k_B T \ln\frac{c_{red}}{c_{ox}} \quad (4)$$

where $E^{(0)}_{redox}$ is the standard redox level for $c_{red} = c_{ox}$. The reduction of the adsorbed molecules at the surface obtained at a small voltage step defines a redox capacitance or pseudocapacitance [11]. This is a particular case of the chemical capacitance $C = e^2 \partial N_i / \partial \mu_i$ [10], which in this case can be expressed as

$$C_{redox} = e^2 \frac{dc_{red}}{dE_{redox}} \quad (5)$$

and from Eq. (4) we get

$$C_{redox} = \frac{e^2 c_{tot}}{k_B T} x(1-x) \quad (6)$$

where x is the fraction of reduced molecules. This capacitance has a bell shape with a maximum value of $e^2 c_{tot}/(4k_B T)$ at $x = 1/2$, corresponding to $V = E^{(0)}_{redox}$, the standard redox potential of viologen.

Therefore, when applying a negative potential (i.e. when the chemical potential of electrons is raised), in the case of the viologen film, the injected charge divides into two branches, one going to charge the chemical capacitance of the semiconductor and the other one filling up the chemical (redox) capacitance of the viologen. If we suppose that this transfer is nearly reversible with respect to interfacial charge transfer, the redox level of viologen will be close to equilibrium with the Fermi level of the semiconductor, $E_{redox} \approx E_{Fn}$. In this case the two chemical capacitors (and the charge that they accumulate) are controlled by the same potential, V, and consequently they are connected in parallel. Thus, the total chemical capacitance of the modified film (and the total charge accumulated on it) is the sum of both contributions while in the case of the bare TiO_2 film, we have only the contribution of the semiconductor and its capacitance is lower.

At the most negative potentials in Fig. 2(a), the capacitance of viologen-activated TiO_2 apparently saturates to a constant value. Two possible reasons can be given for this behaviour. On the one hand, it is possible that the total capacitance of TiO_2 plus viologen rises so much that becomes larger than Helmholtz capacitance at the whole internal surface of the film. In this case, as the electrostatic capacitor in the surface is in series with the chemical capacitance of the film, the smaller will dominate, and the semiconductor enters the state of band unpinning. On the other hand, it is likely that the combination of the exponential increase of the TiO_2 capacitance with the decrease of the viologen capacitance at potentials more negative than $E^{(0)}_{redox}$ also leads, for a certain range of potentials, to a nearly constant capacitance. Data from bare TiO_2 at these potentials, show clearly that Helmholtz limitation is not reached at these potentials. It is thus plausible to assume that the origin of the plateau is the combination of capacitances. At more negative potentials, the viologen covered film is expected to follow nearly the same behaviour as the bare TiO_2, but this region, beyond cathodic potential of -0.8 V, was not investigated to avoid degradation of the film.

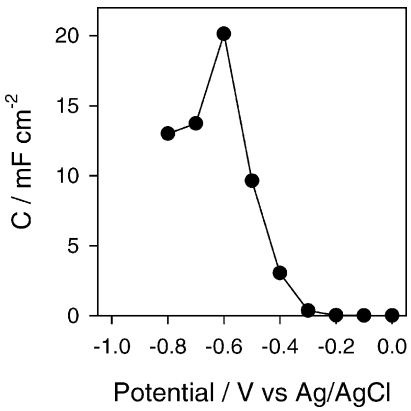

Fig. 3. Redox capacitance of viologen resulting from the subtraction of bare and viologen covered TiO_2 films from Fig. 2(a).

We can now estimate de evolution of the redox capacitance by subtracting the capacitances of bare and viologen-activated TiO_2, Fig. 3. Although this result has to be taken with caution because of possible displacements of the energy levels of TiO_2 related to the absorption of the viologen, the expected bell shape predicted in Eq. (6) is obtained. The maximum, which occurs at the redox potential, is found to be $E^{(0)}_{redox} = -0.6 \pm 0.1$ V. From it we can obtain the lower limit value of $C^{max}_{redox} = 20\,mF\,cm^{-2}$ from which we can estimate $c_{tot} = 3.3 \times 10^{19}\,cm^{-3}$.

If the redox process were not completely reversible, there would exist in Fig. 2(a) certain offset between the electrochemical potentials, E_{Fn} and E_{redox}, related to the charge transfer current between TiO_2 and viologen. It can be shown that this additional physical process leads to modify our previous equivalent circuit model for the viologen system to the one of Fig. 4, in which C_{TiO_2} and C_{redox} are at different potentials, the difference being $E_{Fn} - E_{redox}$, which drives the current through interfacial charge transfer resistance R_{ct}, so that the parallel combination of the redox and semiconductor capacitances is decoupled in the high frequency region. Note that the simpler parallel capacitance model discussed before is obtained in the particular case of Fig. 4 when charge transfer is reversible, $R_{ct} \to 0$. In our measurements, high frequency noise prevented us from determining the presence of this resistance with EIS. We remark also that

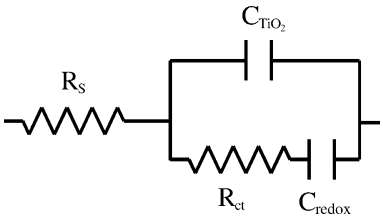

Fig. 4. Proposed impedance model for a viologen modified TiO_2 film in the case of existence of charge transfer resistance, R_{ct}, between the semiconductor and the chromophore. R_S is the series resistance, C_{redox} the capacitance of the viologen and C_{TiO_2} the capacitance of the titanium dioxide film according to the expressions described in the text.

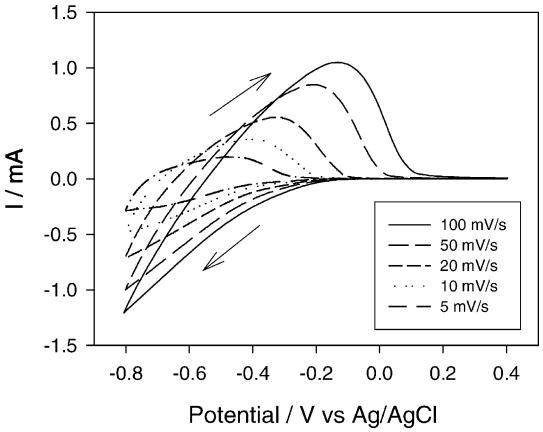

Fig. 5. Voltammetries of the viologen deposited film at different scan rates.

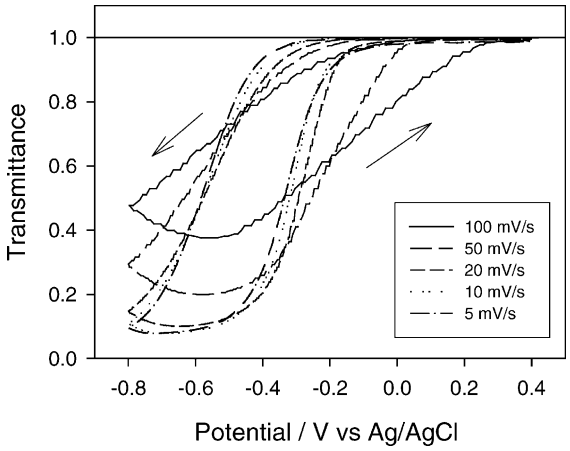

Fig. 6. Transmittance of viologen-activated TiO_2 measured simultaneously to the voltammetries taken at the different scan speeds.

a more complicated situation occurs when the redox potential of the molecules partly shifts when $E_{cb}(TiO_2)$ moves negatively by the change of the Helmholtz potential. The molecule shift depends on the location of the redox centre of the molecule in the adsorbed molecule layer [12].

Cyclic voltammogrames of a viologen-activated TiO_2 film at different scan rates are shown in Fig. 5. The shapes are very similar to those obtained in a previous work and can be simulated with the equivalent circuit models involving capacitances that depend exponentially on the potential, with and without saturation at the constant capacitance value [8]. As stated in that work, the effect of the series resistance, R_S, prevents the film potential (semiconductor Fermi level) to follow exactly the applied potential, because a part of the total potential is taken by the ohmic drop in R_S. This effect is particularly important when large currents are induced, at high scan rates. Therefore, due to R_S, the maximum negative voltage achieved by the film (closest Fermi level position to the lower conduction band edge) during the voltammetry is not the return potential but that at which the current becomes zero for the first time in the return scan. At this moment the film has accumulated the maximum charge and thereafter it begins to be extracted. This is an essential point for understanding the evolution of transmittance, as discussed later on.

The potential at which the capacitance saturates is not reached at the higher scan rates, thus the corresponding voltammogrames only show the effect of the exponentially increasing capacitance. However, at the lower speeds, it can be seen in Fig. 5 that the current tends to a plateau corresponding to the constant capacitance, C_S, obtained by impedance, Fig. 2(a), that leads to the constant current by the relationship $i = C_S s$, where s is the scan rate.

This interpretation of the voltammetries, explains also some of the major features of the transient transmittances obtained at different scan rates, shown in Fig. 6. At the highest rates the potential reached by the film is lower than the potential needed to reduce completely all the viologen. On the contrary, this potential is reached at the lower speeds. This is the reason why the minimum of transmittance decreases with decreasing scan rates and saturates at the lowest of them.

A critical test of this explanation is obtained by comparing the simultaneous transients of electrical current and transmittance on a common scale of potential. As can be seen in Fig. 7, the minimum of transmittance occurs approximately when voltammogram crosses the zero current voltage axis. This is because the minimum of transmittance needs to be delayed from the return potential until the maximum voltage is attained by the film. This delay is larger the greater the scan rate is.

Other facts that show that the processes of injection and extraction of charge are intimately tied to colouring can be observed in Fig. 7. Colouration starts when injection current starts to rise and ends when extraction current vanishes, and furthermore the maximum current coincides, approximately with the maximum slope of the bleaching process. The close relationship between electrical and optical responses is further supported by the frequency domain results of Ref. [4] showing the correspondence of the complex capacitance and modulated transmittance.

Following with this view of our system, we suggest the following description of the processes occurring when

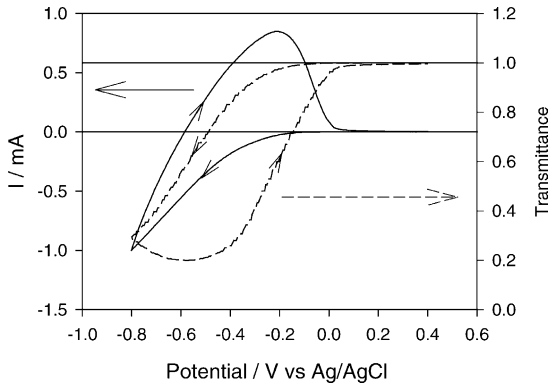

Fig. 7. Comparison of the voltammogram (left axis) taken at a scan rate of 50 mV/s with the transmittance of the film (right axis).

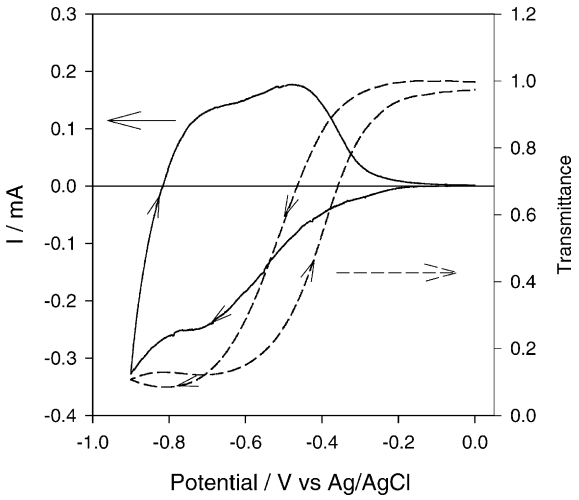

Fig. 8. Comparison of the voltammogram (left axis) taken at a scan rate of 5 mV/s with the transmittance of the film (right axis), when potential is given until values where the viologen starts second reduction.

scanning into more negative potentials at low speeds, Fig. 8. When the potential is first displaced negatively, current and transmittance decrease up to a plateau in current, at the end of which a minimum of transmittance is found. At this potential, the first reduction of viologen has been completed. Note that this plateau corresponds to the constant capacitance found in Fig. 2(a). At more cathodic bias, current becomes more negative and transmittance starts to rise. At this point the second reduction of viologen starts resulting in a less opaque colour (yellow) than the first one (deep blue).

When the turning point of potential is reached, the transmittance continues to increase until current becomes zero, where the more negative potential is reached in the film (as indicated before) and, consequently, a maximum of transmittance is attained. As current becomes positive, the second reduction is reoxidised to first, and transmittance decreases again until it shows a new minimum indicating that reoxidation from twice reduced viologens is overcome (or even finished) by that of viologen once reduced. Thus, from this point reoxidation to the original bleached state dominates and transmittance increases. That neither the second minimum nor the final transmittance have the same magnitudes than their respective original values probably indicates that the second reduction of viologen is not fully reversible. The fact that at potentials more negative than the plateau the current continues rising, is related to the increase of capacitance due to TiO_2 mentioned above and shown in Fig 2(a) as degradation currents, if present at all, are expected to be low at these potentials.

It has to be stressed here that the voltammetry of bare TiO_2 cannot present a reverse peak (i.e. in the scan towards cathodic potentials) due to the characteristic behaviour, of the capacitance of the film: exponential increase until an eventual saturation due to Helmholtz limitation [8]. In our case the voltammetry of the bare TiO_2 sample kept the same shape as that shown in Fig. 9(a) even when the potential was

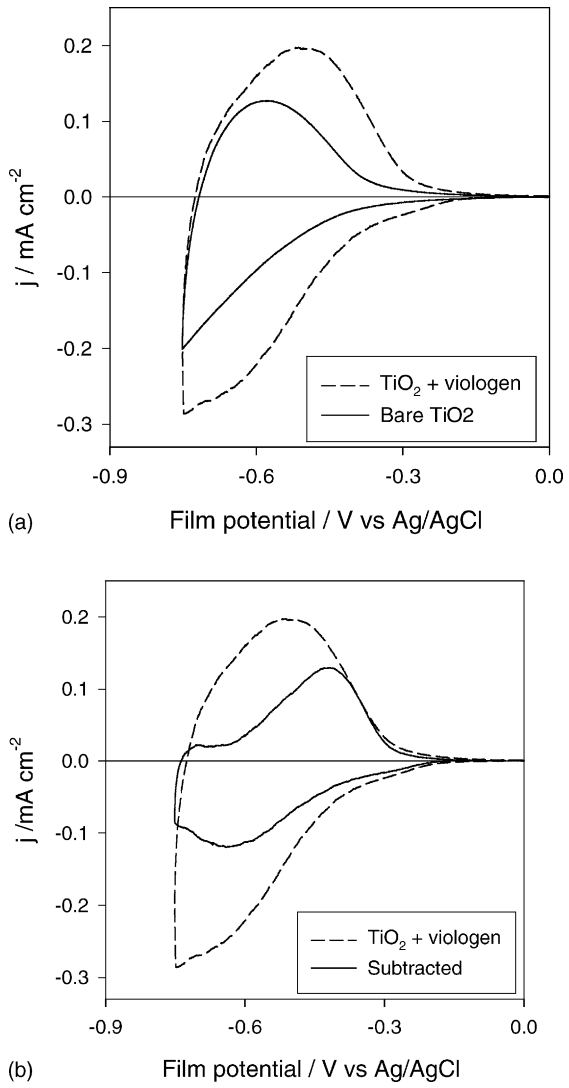

Fig. 9. (a) Voltammetry of viologen derivatised TiO_2 compared to the bare TiO_2 at $s = 5$ mV/s. (b) The same compared to the result of subtraction of normal voltammetries. Film potential is obtained after resistance compensation.

taken as far as −1.1 V (versus Ag/AgCl), never reaching the Helmholtz limit.

As we did before for EIS, we can study the redox process by comparing the the voltammetries of the viologen derivatised film with the bare TiO_2, Fig. 9(a). The subtraction of both voltamogrames, Fig. 9(b), shows a profile similar to the bell-shaped redox process that is predicted by Eq. (6) and Fig. 3. Fig. 9(b) also indicates that the contribution of viologen to the overall electrical capacitive response is very significant. From the maximum of the subtracted voltamogram it is possible to calculate the maximum capacitance of the redox process $C_{\text{redox}}^{\max} = i_{\max}/s = 25\,\text{mF}\,\text{cm}^{-2}$, what agrees very well with the result obtained from EIS. However, as before, these results should be taken with some caution, as absorption of viologen in the surface of TiO_2 can displace the voltammogram in the potential axis.

A better way to see the redox process separately is to treat transmittance data taken during voltammetry: considering that any variation in the transmittance of the film, T, is due to the injection of electrons in the viologen, Beer–Lambert law may be written as

$$A = \varepsilon L \frac{c_{\text{red}}}{N_A} \tag{7}$$

where, neglecting reflectance, $A = -\ln(T)$ is the absorbance, ε the molar absorption coefficient of reduced viologen and L the film thickness.

If we derive this expression with respect to the potential and take into account that for cyclic voltammetry $\mathrm{d}V = s\mathrm{d}t$, we obtain

$$\frac{\mathrm{d}A}{\mathrm{d}V} = \frac{\varepsilon L}{N_A}\frac{\mathrm{d}c_{\text{red}}}{\mathrm{d}V} = \frac{\varepsilon L}{sN_A}\frac{\mathrm{d}c_{\text{red}}}{\mathrm{d}t} \tag{8}$$

being $\mathrm{d}c_{\text{red}}/\mathrm{d}t$ the variation of reduced viologens with time or, in other words, the current density, j, that enters viologen molecules divided by the electron charge and the length of the film. Thus Eq. (8) yields [13]

$$s\frac{\mathrm{d}A}{\mathrm{d}V} = \frac{\varepsilon}{F}j \tag{9}$$

where F is the Faraday constant. Alternatively, the first equality of Eq. (8) when compared with Eq. (5) shows that $\mathrm{d}A/\mathrm{d}V \propto C_{\text{redox}}$, i.e. the derivative of the absorbance reveals the capacitance of the redox process completely separated from the TiO_2 capacitance contribution. We note that the contribution of Li^+ insertion to coloration of the TiO_2 film can be neglected. It was measured to be less than 10% at the most negative potentials over the bare TiO_2.

In Fig. 10 we plot the optical determination of the redox process of viologen, Eq. (9), and compare it with the result of the electrical technique obtained previously from subtraction in Fig. 9(b). Good agreement is found between both representations of the redox process, though the optical method provides the clearest result. Thus, the cathodic and anodic peak potentials can be computed readily, $V_{\text{pc}} = -0.63\,\text{V}$ and $V_{\text{pa}} = -0.45\,\text{V}$, respectively, what indicates that the process is not completely reversible at these scan rates yielding a standard redox potential $E^{(0)}_{\text{redox}} = -0.54 \pm 0.02\,\text{V}$ versus Ag/AgCl. This value lies inside the window given by EIS data and 50 mV more positive than that found in a 0.2 M $LiClO_4$ in γ-butyrolactone electrolyte [2]. The partial irreversibility of the redox process at low speeds can be understood as the separation between the electrochemical potentials, E_{Fn} and E_{redox}, due to kinetic limitations in the charging of viologen, in other words, to the charge transfer resistance proposed in the model of Fig. 4.

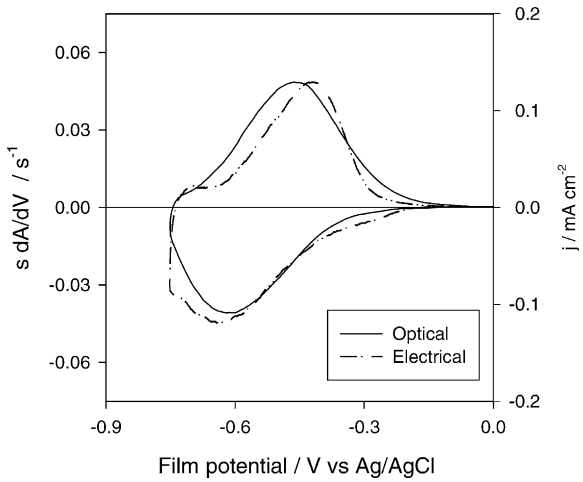

Fig. 10. Comparison of the decoupling of the redox process of viologen by the electrical and optical methods. Right axis: subtracted electrical voltammetry obtained in Fig. 9(b). Left axis: derivate of absorbance times scan rate (5 mV s^{-1}).

A value of the molar absorption coefficient $\varepsilon = 3.7 \times 10^4\,\text{M}^{-1}\,\text{cm}^{-1}$ was estimated from the scaling of Fig. 10. Though this value is comparable to those that can be extrapolated from figures of [2,3], respectively, it has to be taken with care as the subtraction we have made to obtain the redox response of Fig. 9(b) is very sensible to the eventual shifts in the potential indicated above.

Assuming this value of ε and that at all the viologens are in the first reduced state at the minimum of transmittance of Fig. 8, through Eqs. (6) and (7) we estimated the concentration of adsorbed viologen $c_{\text{tot}} = 10.2 \times 10^{19}\,\text{cm}^{-3}$ ($C^{\text{max}}_{\text{redox}} = 63\,\text{mF}\,\text{cm}^{-2}$), which is of the same order of magnitude obtained previously.

An improvement of our methods to give a more reliable value of ε and thus of c_{tot} and $C^{\text{max}}_{\text{redox}}$ is in progress. Our results also open a number of questions that will be investigated in future work. It appears worthwhile to investigate in more detail the kinetics of interfacial electron transfer between TiO_2 and the molecules attached to the surface.

4. Conclusions

Viologen-activated TiO_2 behaves electrically as a capacitor with a characteristic potential dependence, in series with a resistance mainly due to electrolyte and FTO substrate contributions. At the measured potentials this capacitance is the result of the sum of the Helmholtz capacitance of the uncovered FTO bottom layer (which plays a minor role), and a chemical capacitance that depends on the potential through two contributions: charge accumulation in TiO_2 and the redox capacitance that accounts for the charge injected on the viologen attached in the surface of TiO_2. Helmholtz layer limitation to capacitance was not found in the present study.

This simple model allows to explain the correlation among impedance, voltammetry and transient transmittance data in terms of the time-varying potential applied to the film, that controls the injection of charge through the modulation of the Fermi level in the semiconductor matrix.

The dynamic response of viologen-activated TiO_2 has been described separating the viologen redox process from the overall response of the system. The interfacial charge

transfer process is not completely reversible, and the standard redox potential is −0.54 V versus Ag/AgCl. Furthermore, the contribution of viologen reduction to the electrical response seems to be rather significant until colouration (redox process) is completed.

Acknowledgements

This work was supported by Fundació Caixa-Castelló (projects P11B2002-39 and 02G014.31/1) and the Swedish Research Council.

References

[1] D. Cummins, G. Boschloo, M. Ryan, D. Corr, S.N. Rao, D. Fitzmaurice, J. Phys. Chem. B 104 (2000) 11449.
[2] R. Cinnsealach, G. Boschloo, N.S. Rao, D. Fitzmaurice, Sol. Energy Mater. Sol. Cells 57 (1999) 107.
[3] P. Bonhote, E. Gogniat, F. Campus, L. Walder, M. Grätzel, Displays 20 (1999) 137.
[4] J. Garcia-Cañadas, L.M. Peter, U.K.G. Wijayantha, Electrochem. Commun. 5 (2003) 199.
[5] M.O.M. Edwards, T. Gruszecki, H. Pettersson, G. Thuraisingham, A. Hagfeldt, Electrochem. Commun. 4 (2002) 963.
[6] I. Abayev, A. Zaban, F. Fabregat Santiago, J. Bisquert, Phys. Stat. Sol. (a) 196 (2003) R4.
[7] F. Fabregat-Santiago, G. Garcia-Belmonte, J. Bisquert, A. Zaban, P. Salvador, J. Phys. Chem. B 106 (2002) 334.
[8] F. Fabregat-Santiago, I. Mora-Seró, G. Garcia-Belmonte, J. Bisquert, J. Phys. Chem. B 107 (2003) 758.
[9] F. Fabregat-Santiago, G. Garcia-Belmonte, J. Bisquert, P. Bogdanoff, A. Zaban, J. Electrochem. Soc. 150 (2003) E293.
[10] J. Jamnik, J. Maier, Phys. Chem. Chem. Phys. 3 (2001) 1668.
[11] B.E. Conway, Electrochemical Supercapacitors, Plenum Publishing, New York, 1999.
[12] A. Zaban, S. Ferrere, B.A. Gregg, J. Phys. Chem. B 102 (1998) 452.
[13] S.L.D. Maranhâo, R.M. Torresi, Electrochim. Acta 43 (1998) 257.